

## **A Functional-Structural Model of Chrysanthemum for Prediction of Ornamental Quality**

P.H.B. de Visser, G.W.A.M. van der Heijden  
and L.F.M. Marcelis  
Plant Research International  
P.O. Box 16  
6700 AA Wageningen  
The Netherlands

S.M.P. Carvalho and E. Heuvelink  
Horticultural Production Chains Group  
Wageningen University  
Marijkeweg 22  
6709 PG Wageningen  
The Netherlands

**Keywords:** L-system, physiological model, virtual plant, sink strength, flower quality

### **Abstract**

**An integration of structural and physiological models is used to simulate 3D plant growth and visual appearance of cut chrysanthemum, reacting on environmental factors. Measurements to calibrate the model include 3D data of digitised plants as well as a number of measurements and observations on harvested plants, including biomass per organ. The structural module is based on the L-systems algorithm. This L-system calculates temperature and light driven development, branching pattern, and flower formation. In this 3D structural model existing rules for physiological processes are incorporated, enabling calculation of carbon dynamics. A 3D radiosity method is used to calculate light absorption of every organ (leaf) at an hourly basis. Hourly photosynthesis per leaf is calculated according to the biochemical model of Farquhar taking into account absorbed light, CO<sub>2</sub>, and temperature at hourly intervals. A relative sink strength approach is used to distribute the available assimilates among organs at a daily basis.**

**Simulated growth response to temperature is based on various trial data. Modelling of light interception and photosynthesis is currently tested for one plant density only. Since the 3D crop consists of a set of individual plants, simulation of plant to plant competition for light is enabled. The model is able to visualise different flower qualities in terms of flower number, flower size and branching patterns per plant. The results show the effects of local growth of organs on the structure and ornamental quality at plant level.**

### **INTRODUCTION**

A number of studies have shown the usefulness of explanatory models in simulating the interactions of climate and management on ornamental quality and quantitative properties of chrysanthemum plants (Carvalho and Heuvelink, 2003; Lee and Heuvelink, 2003; Larsen and Gertsson, 1992). Those models all operate at the plant level, and do not explicitly simulate 3D plant structure although they may be able to discriminate between individual organs using a ranking or index. Moreover, physiological processes that relate to structure cannot be modelled explicitly, for example light absorption on individual leaves or flow of substances and signals. Here, we present a prototype functional-structural plant model (FSPM) for cut chrysanthemum that possesses some of these features in order to model ornamental quality in response to abiotic conditions. Only a few studies have incorporated and visualised 3D plant structures in mechanistic growth models up to now (for an overview, see Godin and Sinoquet, 2005). Especially the L-system formalism (Lindenmayer and Prusinkiewicz, 1990) is able to generate detailed, realistically visualised 3D plants in interaction with their 3D environment, and are referred to as 'virtual plants' (e.g. Room et al., 1996). This approach is used in this study for cut chrysanthemum cultivar 'Reagan Improved' and extended with rules from process-based physiological models. Recent studies show that simultaneous modelling of structures and functions can explicitly model the effects of local processes on the plant and crop level (e.g. Drouet and Pagès, 2003). In this paper, such a combination is used for light and temperature effects on development and growth

of individual organs. The model is parameterised by data derived from a growth trial under controlled conditions.

## METHODS

### Model Description

The model consists of three modules:

- An architectural module, describing the spatial relation and development of the plant-organs in terms of symbols, according to the L-alphabet (e.g. Lindenmayer and Prusinkiewicz, 1990).
- A light-interception module, which takes as input the 3D-scene, including the position and intensity of photosynthetic active radiation (PAR) of the light sources. The nested radiosity model, developed by Chelle and Andrieu (1998), is used to calculate the absorbed PAR at every leaf.
- A carbon module, which consists of two sub-modules:
  - a. an assimilation module according to the biochemical model of Farquhar (Farquhar et al., 1980), which calculates the hourly produced amount of assimilates per leaf.
  - b. a sink/source module, which takes into account the maintenance respiration and the assimilate distribution over the various plant organs according to a relative sink strength model. The hourly assimilation per leaf is aggregated to plant level each day and distributed over the plant.

**1. Inputs.** Environmental conditions are supplied to the model as hourly readings of PAR intensity (in  $\mu\text{mol photons m}^{-2} \text{ s}^{-1}$ ) and spatial position, temperature, global  $\text{CO}_2$  concentration and global relative humidity. From the hourly data, the night length is determined, which is relevant for inducing the generative phase of this short-day plant species. The mean day temperature is determined from the 90%-percentile of hours with light levels sufficient for growth.

**2. Development.** The architectural model starts by generating an L-system of a young stem cutting with visible leaves and a number of ‘hidden’ phytomers, not visible by eye. During vegetative development axillary meristems (one internode, leaf and axillary bud each) on the main stem are initiated in an acropetal gradient (from base to top of plant). A base temperature of  $0^\circ\text{C}$  is used for all physiological processes (Larssen and Gertsson, 1992). The generative phase starts at the first occurrence of a night length longer than 11 hours. A terminal flower bud is formed, breaking apical dominance. Next, axillary buds on the main stem will develop to side shoots with flowers in a basipetal direction, i.e. from top towards base. Every elongating side shoot will develop one flower, and more flowers may occur if the simulated carbohydrate reserves will reach a certain level.

In brief (for details, see De Visser et al., 2006), the temperature dependent processes in the model are: phytomer appearance rate and internode elongation rate (also side shoots), lag time between start of short-day period and (terminal) flower evocation, rate of side shoot appearance, organ growth rate, photosynthesis, maintenance. These processes show either an incremental response to temperature or have an optimum at ca.  $20^\circ\text{C}$ .

Growth processes modelled from interaction between temperature and assimilate supply are: activation of dormant buds, organ growth rate, internode length and flower size.

**3. Photosynthesis.** For photosynthesis modelling, PAR intensity and direction is calculated from global radiation and position of sun and/or assimilation light at the hemisphere. The L system receives data on light level per leaf from the coupled nested radiosity model. Reflection of PAR is derived from experiments, and downward and upward transmission was assumed 10% (Goudriaan and Van Laar, 1994) and 0% respectively. Photosynthesis is calculated according to the biochemical model of Farquhar et al. (1980) on basis of absorbed light,  $\text{CO}_2$ , and temperature at hourly intervals. The initial light use efficiency  $\alpha$  and maximum electron transport rate  $J_{max}$  are derived from the experimental data (see below). Details on the modelling approach are given by De Visser et al. (2006).

**4. Carbohydrate Dynamics in the Plant.** The carbohydrates from net photosynthesis of individual leaves are added at plant level to the pool of available carbohydrates. The carbohydrate modelling follows the approach of relative sink strength (Marcelis, 1996). Details on the modelling are presented in De Visser et al. (2006). The sink strength of the organs is derived from dry matter increment as a function of the weighted temperature sum using a Gompertz curve. The derivative of the Gompertz curve gives the sink strength at a certain weighted thermal time. For model parameterisation, the sink strength was determined empirically on all the data.

**5. Allometry and 3D Structure.** The model has to be supplied with quantitative relationships between weight-length and weight-area for leaves, between weight-length, weight-width and weight-volume for internodes, and between weight-area for flowers. Also model input is phyllotaxis of the leaves on the main stem, azimuthal angle of leaves and flowering shoots, and leaf shape.

### **Plant Measurements**

**1. Experiment.** In a growth chamber experiment, stem cuttings of chrysanthemum cultivar 'Reagan Improved' were planted in 12 cm pots at a density of 69 plants per m<sup>2</sup>. Two temperature treatments were carried out, 16°C and 20°C each in a replicated growth chamber at a relative humidity of 75% (16°C) and 70% (20°C). The experiment lasted 70 (20°C) to 77 (16°C) days. Plants were grown under long day (LD period) condition for 14 days, followed by short day (SD period) until the end of the experiment. During the LD and SD period assimilation light of 370 μmol PAR m<sup>-2</sup> s<sup>-1</sup> was provided for 8 hrs, extended with incandescent lamps (13 μmol) for 11 hrs in LD and 3 hrs in SD period. Light extinction was measured with light sensors (n=6) placed above and below the canopy on the dates of the destructive harvests and related to the observed LAI.

**2. Collection of Plant Data by Destructive Harvests.** At the start of the experiment, at the end of the LD period, two times during the SD period and at the final harvest, 5 plants per treatment were harvested for determination of organ length, internode thickness, individual leaf and flower areas, organ fresh and dry weight (dried at 105°C for 48 hours) and leaf shape. Tests on treatment differences and curve fitting performed with the Genstat statistical package.

**3. Sink Strength.** The observed rates of biomass increment with thermal time of internodes, leaves and flowers were used to determine the parameters of the sink strength curve. Internode and leaf data on phytomers 9 to 20 of the plants were used, assuming no competition for carbon sources during organ formation in this exponential growth phase. The sink function for flowers is forced to a maximum biomass of 0.21 g DM, which was observed for potential flower growth of this cultivar (Carvalho et al., 2003).

**4. Collection of 3D Data.** A Scanstation (Turnbull, Germany) was used to digitize the 5 plants in 3D prior to their harvest (for method details see De Visser et al., 2006).

## **RESULTS**

### **General Growth Aspects**

The newly formed leaves and internodes reached a higher weight and size than those that were present at the start. A considerable amount of phytomers were not visible by eye at the experimental start. From the final number of leaves and a leaf appearance rate of 0.6 leaf per day at 20°C we calculated backwards a total of 22 phytomers present at the start of the experiment.

### **Sink Strength Estimation**

Leaves reached their maximum growth rate earlier than flowers and internodes. The sink strength functions, derived from the weight increments, clearly show this pattern (Fig. 1). Although internodes grew in length equally fast as leaf length and leaf weight, their weight increase, and derived sink strength, lagged behind, indicating an increasing specific weight of internodes with thermal time.

Assimilate production was tuned to arrive at the observed total biomass at both temperatures. Carbohydrate allocation modelled according to the relative sink strength was initially not correct for the generative phase, due to a too rapid start of the flower sinks. So, for modelling the correct number and weights of flowers, the delay in flower formation after SD start at 16°C relative to the 4.3 days at 20°C was tuned, keeping an equal threshold assimilate level of 1.5 g CH<sub>2</sub>O per plant for both temperatures. The delay was found to be 18 days after start of the SD period. Subsequently, observed and modelled allocation agreed fairly well (Table 1).

### Photosynthesis

The simulated plant development, tuned above, was used to compare and adjust simulated light attenuation in the canopy, resulting in a PAR reflection of 10% by leaves. With the resulting light absorption, the initial estimates of the photosynthesis parameters  $\alpha$  and  $J_{max}$  were adjusted to arrive at good fits between simulated and observed dry matter increment during linear growth, i.e. from 25 to 50 days after treatment start, at constant light input of 13.4 mol PAR m<sup>-2</sup> d<sup>-1</sup>. We obtained an  $\alpha$  of 0.75  $\mu$ mol electron per  $\mu$ mol PAR.  $J_{max}$  was adjusted to 320  $\mu$ mol e m<sup>-2</sup> s<sup>-1</sup>.

### Allometry and Structure

A mean leaf angle and phyllotaxis of 40° ( $\pm$ 15°) respectively 135° ( $\pm$ 32°) was observed. The allometric relationships were:

$$\text{internode: length (mm)} = 260 * \text{weight} - 632 * \text{weight}^2 \quad (\text{i})$$

$$\text{internode: width (mm)} = 2 + 30 * \text{weight} \quad (\text{ii})$$

$$\text{leaf: length (mm)} = 337.0 * \text{weight}^{0.48} \quad (\text{iii})$$

$$\text{leaf: area (cm}^2\text{)} = 329.0 * \text{weight} \quad (\text{iv})$$

$$\text{flower: diameter (mm)} = 552.36 * \text{weight} - 881.61 * \text{weight}^2 \quad (\text{v})$$

No significant differences of SLA between temperature treatments were found, enabling the use of formula iv for simulation of the experiments.

Thus, organ weights are converted to 3D dimensions, to be used in L-string generation for visualization (Fig. 2) and light capturing.

### Observations versus Model Simulations

In the growth chamber experiment, differences at plant level between temperature treatments were significant for plant height and flower biomass (Table 1). There were trends towards a higher number of flowers, a lower leaf mass and leaf area at 20°C relative to 16°C. At the organ level internodes were shorter and thicker and leaves were larger for 16°C relative to 20°C. At an equal number of flowers, plants at 20°C started flowering earlier than at 16°C, resulting in a stronger allocation of carbohydrates to flowers at the expense of stem and leaves. The model correctly simulated this higher allocation to flowers (Table 1) and also simulated lower weights of individual flowers at the lower temperature (Fig. 3). The distribution of mass within the stem showed a pattern as observed (Fig. 4).

### DISCUSSION

The model is able to simulate the influence of temperature and assimilate level at organ level and on plant appearance and ornamental quality in terms of stem width, stem height and flower size. Calibration was performed on two temperature treatments only, so the model's behaviour under changing growth conditions has to be explored further. Moreover, some temperature effects on growth were not observed, where one should expect increased flower weight (Van der Ploeg et al., 2005) and decrease of SLA (Acock et al., 1979) at lower temperature, making correct calibration difficult. Therefore, additional data gathering in greenhouse experiments at different temperatures and planting densities is planned for validation.

Our use of simulated 3D light absorption at leaf level might not be required since our model pools the produced assimilates at plant level. Moreover, a 3D light model like

the applied radiosity method requires complicated measurements on direction and intensity of the light sources and subsequent interception by the plant. Yet, modelling local differences in light absorption per leaf can potentially be helpful to explain effects of local situations on plant development, like the tillering behaviour of wheat (Evers et al., 2005) or the breaking of rose buds.

Chrysanthemum growers have many options to adapt their greenhouse environment and thus challenge the modellers to incorporate many growth mechanisms. However, even combined effects of radiation and temperature are difficult to quantify, e.g. at higher radiation levels, sensitivity to higher temperature decreases, or, at lower radiation levels, start of flower initiation is retarded at low temperature (Karlsson et al., 1989). Further knowledge on chrysanthemum growth at a wider range of cultivars and environmental conditions has to be incorporated in the model to make it useful for decision support of growers. Nevertheless, the model can be advocated as an attractive and innovative tool because now ornamental quality can be visualised in 3D.

#### Literature Cited

- Acock, B., Charles-Edwards, D.A. and Sawyer, S. 1979. Growth response of a *Chrysanthemum* crop to the environment. III, Effects of radiation and temperature on dry matter partitioning and photosynthesis. *Ann. Bot.* 44:289-300.
- Carvalho, S.M.P. and Heuvelink, E. 2003. Effect of assimilate availability on flower characteristics and plant height of cut chrysanthemum: an integrated study. *J. Hort. Sci. Biotechnol.* 78(5):711-720.
- Carvalho, S.M.P., Heuvelink, E., Harbinson, J. and Van Kooten, O. 2003. Effect of sink-source ratio and flower position on chrysanthemum flower size. *Phys. Plant.*
- Chelle, M. and Andrieu, B. 1998. The nested radiosity model for the distribution of light within plant canopies. *Ecol. Modelling* 111:75-91.
- De Visser, P.H.B., Van der Heijden, G.W.A.M., Heuvelink, E. and Carvalho, S. 2006. Functional-structural modeling of chrysanthemum. In: J.A. Vos and L.F.M. Marcelis (eds.), *Functional-structural plant modelling in crop production*, Kluwer Academic Publishers, The Netherlands (in press).
- Drouet, J.-L. and Pagès, L. 2003. GRAAL: a model of growth, architecture and carbon allocation during the vegetative phase of the whole maize plant. Model description and parameterisation. *Ecol. Modelling* 165:147-173.
- Evers, J.B., Vos, J., Fournier, C., Andrieu, B., Chelle, M. and Struik, P.C. 2005. Towards a generic architectural model of tillering in Gramineae, as exemplified by spring wheat (*Triticum aestivum*). *New Phytol.* 166(3):801-812.
- Farquhar, G.D., Von Caemmerer, S. and Berry, J.A. 1980. A biochemical model of photosynthetic CO<sub>2</sub> assimilation in leaves of C<sub>3</sub> species. *Planta* 149:78-90.
- Godin, C. and Sinoquet, H. 2005. Functional-structural plant modelling. *New Phytol.* 166:705-708.
- Goudriaan, J. and Van Laar, H.H. 1994. *Modelling potential crop growth processes: textbook with exercises. Current issues in production ecology 2.* Dordrecht: Kluwer Academic Publishers. 238p.
- Karlsson, M.G., Heins, R.D., Erwin, J.E., Berghafe, R.D., Carlson, W.H. and Biernbaum, J.A. 1989. Temperature and photosynthetic photon flux influence chrysanthemum shoot development and flower initiation under short-day conditions. *J. Amer. Soc. Hort. Sci.* 114:158-163.
- Larsen, R. and Gertsson, U. 1992. Model analysis of shoot elongation in *Chrysanthemum x morifolium*. *Sci. Hort.* 49:277-289.
- Lee, J.H. and Heuvelink, E. 2003. Simulation of leaf area development based on dry matter partitioning and specific leaf area for cut chrysanthemum. *Ann. Bot.* 91(3):319-327.
- Marcelis, L.F.M. 1996. Sink strength as a determinant of dry matter partitioning in the whole plant. *J. Exp. Bot.* 47:1281-1291.
- Lindenmayer, A. and Prusinkiewicz, P. 1990. *The algorithmic beauty of plants.* New York, Springer-Verlag.

- Room, P.M., Hanan, J.S. and Prusinkiewicz, P. 1996. Virtual plants: new perspectives for ecologists, pathologists and agricultural scientists. *Trends in Plant Science* 1:33-38.
- Van der Ploeg, A., Smid, H.G. and Heuvelink, E. 2005. Cultivar differences in temperature demand of cut chrysanthemum. *Acta Hort.* 691:91-98.

## **Tables**

Table 1. Observed (n = 5) and simulated total biomass of organs (g plant<sup>-1</sup>, including side shoots) and plant characteristics at the end of the growth chamber experiment. Different letters behind means indicate differences at 5% level between treatments.

	16°C		20°C	
	Observed	Model	Observed	Model
Weight leaves	3.1 ± 0.3	2.9	2.8 ± 0.6	2.8
Weight internodes	6.2 ± 1.1	6.1	6.0 ± 1.4	5.9
Weight flowers	2.0 ± 0.4a	2.1	2.8 ± 0.6b	2.8
Total	11.3 ± 1.5	11.1	11.6 ± 2.8	11.5
Plant height (cm)	65 ± 5a	77	76 ± 3b	76
Leaf area (cm <sup>2</sup> )	1154 ± 61	953	1018 ± 229	920
Nr of leaves#	33 ± 1.6	33	33 ± 1.5	33
Nr of flowers	20 ± 4	17	23 ± 7	22

# leaves from main stem only

## Figures

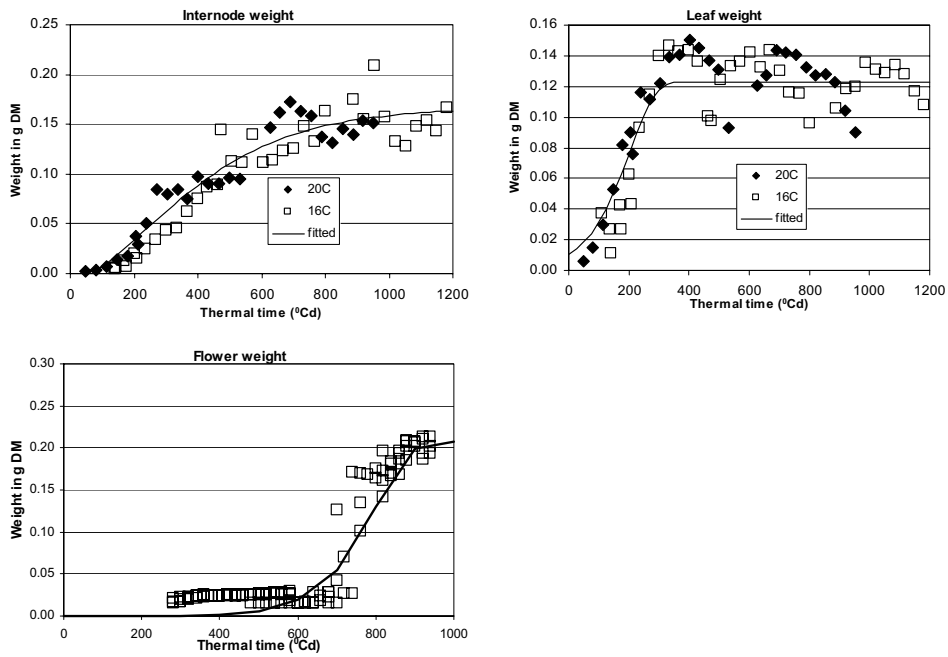


Fig. 1. Biomass increment (in g DM) of organs with thermal time, and fitted with a Gompertz curve. Organs were located on phytomers 10 to 20 of 5 plants. Except for flowers, observed values from the two temperature treatments have different symbols. Explained variance was 95.6 (leaves), 92.0 (internodes) and 87.9% (flowers).

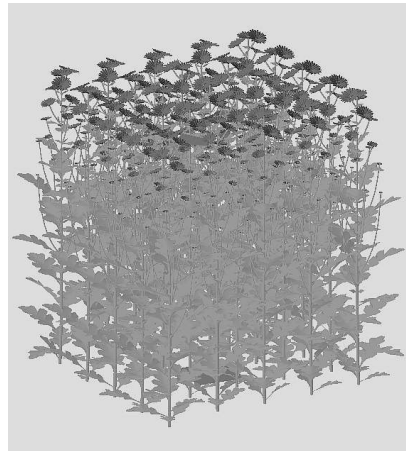


Fig. 2. Simulated chrysanthemum crop after 70 days at 20°C in the growth chamber experiment.

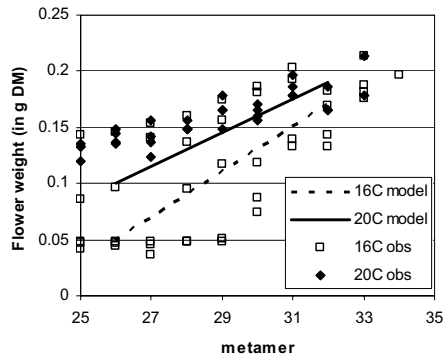


Fig. 3. Distribution of average flower weight along the main stem. Blocks, 16°C; diamonds, 20°C.

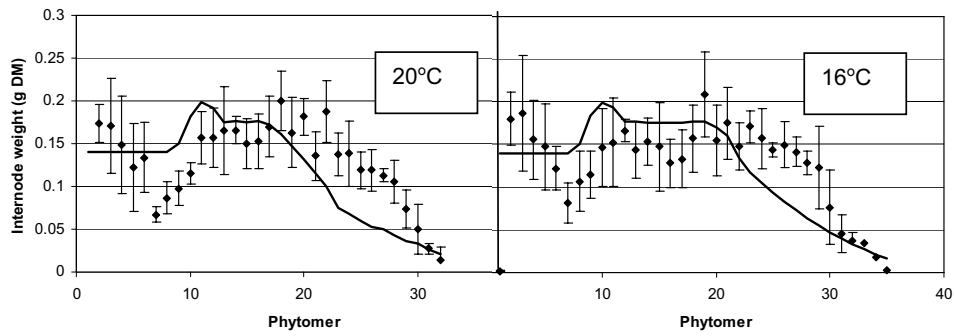


Fig. 4. Observed (symbols) and simulated (lines) internode weight (in g DM) at final harvest.